Biol. Cybern. 76, 257–273 (1997)

Biological Cybernetics

Self-organization of trajectory formation

I. Experimental evidence

J. J. Buchanan [1,2], **J. A. S. Kelso** [1], **G. C. de Guzman** [1]

[1] Program in Complex Systems and Brain Sciences, Center for Complex Systems, Florida Atlantic University, Boca Raton, FL 33431, USA
[2] R. S. Dow Neurological Sciences Institute, Legacy Good Samaritan Hospital and Medical Center, 1120 N.W. 20th Ave., Portland, OR 97202, USA

Received: 2 February 1996 / Accepted in revised form: 13 December 1996

Abstract. Most studies examining the stability and change of patterns in biological coordination have focused on identifying generic bifurcation mechanisms in an already active set of components (see Kelso 1994). A less well understood phenomenon is the process by which previously quiescent degrees of freedom (*df*) are spontaneously recruited and active *df* suppressed. To examine such behavior, in part I we study a single limb system composed of three joints (wrist, elbow, and shoulder) performing the kinematically redundant task of tracing a sequence of two-dimensional arcs of monotonically varying curvature, κ. Arcs were displayed on a computer screen in a decreasing and increasing κ sequence, and subjects rhythmically traced the arcs with the right hand in the sagittal plane at a fixed frequency (1.0 Hz), with motion restricted to flexion-extension of the wrist, elbow, and shoulder. Only a few coordinative patterns among the three joints were stably produced, e.g., in-phase (flexion-extension of one joint coordinated with flexion-extension of another joint) and antiphase (flexion-extension coordinated with extension-flexion). As κ was systematically increased and decreased, switching between relative phase patterns was observed around critical curvature values, κ_c. A serendipitous finding was a strong 2:1 frequency ratio between the shoulder and elbow that occurred across all curvature values for some subjects, regardless of the wrist-elbow relative phase pattern. Transitions from 1:1 to 2:1 frequency entrainment and vice versa were also observed. The results indicate that both amplitude modulation and relative phase change are utilized to stabilize the end-effector trajectory. In part II, a theoretical model is derived from three coupled nonlinear oscillators, in which the relative phases (ϕ) between the components and the relative joint amplitudes (ρ) are treated as collective variables with arc curvature as a control parameter.

Correspondence to: J. A. S. Kelso, Florida Atlantic University, Center for Complex Systems, P.O. Box 3091, Boca Raton, FL 33431-0991, USA (Fax: + (407) 367-3634)

1 Introduction

Everyday actions involving the arm such as lifting, tracing, and pointing are performed effortlessly despite (or perhaps because of) the fact that a very large number of degrees of freedom (neurons, muscles, joints) are coordinated in a task-specific fashion. The question of how such movements are accomplished has been investigated using tasks involving movements of either single (e.g., Asatryan and Feldman 1965; Feldman 1986; Kelso 1977; Polit and Bizzi 1978) or multiple joints (e.g., Kelso et al. 1979; Lacquaniti and Soechting 1982; Lacquaniti et al. 1986; Soechting and Lacquaniti 1981). In the latter but not the former case, an ambiguity exists between trajectories in joint coordinates and the position of the end effector in extrinsic coordinates. That is, the limb has redundant degrees of freedom, and thus constraints must arise naturally or be imposed artificially in order to eliminate such degeneracy (Bernstein 1967). The precise level of the underlying control system at which constraints are thought to apply depends on the methodology adopted (Stein 1982) and may be investigated at several related levels of analysis, e.g., neurophysiological, biomechanical, and behavioral.

Although the so-called Bernstein degrees of freedom problem may be framed in terms of discovering the appropriate central variable controlled by the neurophysiological system (for review see Latash 1993), this article presents evidence that general principles of coordination emerge when the motion produced is treated as a solution of a dynamical system. Let us disregard for the moment the time evolution of a system composed of the wrist, elbow, and shoulder joints and concentrate on the end-effector (e.g., a finger or hand-held instrument) to joint space mapping. It has been rigorously shown (Klein and Huang 1983) that this mapping is ill defined because the joint angles are not functions of the end-effector position. Thus, for a given end-effector position, there are, in principle, an infinite number of wrist, elbow, and shoulder joint angle combinations which may satisfy that static position. This indeterminism, however, is partly resolved when the system is allowed to evolve in time in

the performance of the task, i.e., becomes a dynamical system. Under certain circumstances, as the end-effector travels on a trajectory, stable phase relationships may exist between the joint angle variables. For example, Soechting, Lacquaniti and Terzuolo (1986) found that a phase difference of 180° is maintained between the forearm and upper arm elevation angles when circles and ellipses are drawn on the sagittal and frontal planes. Even though specifically defined static mappings between the arm configuration and the end point do not exist, constraints may arise when the task is performed continuously over time (Soechting and Terzuolo 1987a, b). Such results suggest that temporal constraints play an important functional role in the assembly of single-limb, multijoint movements (e.g., Kelso et al. 1991).

Temporal constraints have played an important role in identifying collective variables and their dynamics (equations of motion) that govern the formation and change of behavioral patterns in a variety of coordination tasks, e.g., interlimb (Kelso 1981, 1984; Treffner and Turvey 1995; Walter and Swinnen 1990, 1992) and multilimb (Carson et al. 1995; Jeka and Kelso 1995) coordination, single-limb multijoint movements (Buchanan and Kelso 1993; Kelso et al. 1991, 1994a), and two-person coordination (Amazeen et al. 1995; Schmidt and Turvey 1994; Schmidt et al. 1990). In each of the above experimental systems, relative phase and its associated variability have successfully described the coordination dynamics (stability, loss of stability, pattern switching, etc.) of the observed behavior (e.g., Haken et al. 1985; see Schöner and Kelso 1988 for review). In addition to its effectiveness in accounting for the coordination of action, relative phase also qualitatively demarcates differences between visually detected patterns, for example, those specified by the acts of walking, running, or moving the arm (e.g., Kelso and Pandya 1990; Haas et al. 1991; Haken et al. 1990). This temporal constraint is characteristic of a coordinative structure or functional linkage, where the control of many individual degrees of freedom is reduced to that of a simpler lower-dimensional dynamic.

Most of the foregoing research has dealt with pattern stability and change in an already active set of participating components. However, in some situations biological systems spontaneously recruit previously inactive components to maintain a pattern of movement. For example, quadrupeds go through a series of stable gait patterns (walk, trot, etc.) as speed is increased. Once the animal starts to gallop, further increases in speed are maintained but with a noticeable backbending (recruitment of the vertical *df*, e.g., see Grillner 1975). Kelso et al. (1993) (see also Buchanan et al. 1997; Kelso and Scholz 1985) have shown that in coordinated motions involving adduction and abduction of the index fingers in the horizontal plane, spontaneous transitions from asymmetrical patterns (homologous muscles contracting alternately) to symmetrical patterns (homologous muscle contracting together) occur as the frequency f of the oscillation reaches a critical value, f_1. Following this transition, the fingers move from the x-plane to the y-plane at a second critical frequency, $f_2 > f_1$, regardless of the initial coordination pattern. Similar to the case of the galloping quadruped, the recruitment of a quiescent degree of freedom provides a mechanism for maintaining stability in a system when the current area of its phase space no longer provides alternative stable states. This sudden or gradual recruitment of vertical motion (and subsequent annihilation of horizontal motion) corresponds to a Hopf bifurcation from a fixed point to limit cycle attractor and vice versa (Kelso et al. 1993).

As the above work demonstrates, scaling on a system-sensitive parameter (here the movement frequency) may elicit the recruitment of quiescent *df* in order to maintain a stable task-specific coordinative pattern. Many movements, however, may be characterized in terms of both temporal and spatially defined constraints. Changing the spatial aspect of a task may also induce the recruitment and suppression of *df*, as seen, for example, in reaching tasks when the subject-to-object distance varies or the orientation of an object changes suddenly (e.g., Kelso et al. 1994a). In such a scenario, depending on object distance or orientation, a subject may either employ just a limb or a limb and the torso when reaching. Motivation for the experiment presented here was derived from previous work by Kelso et al. (1991) in which two stable phase relationships between the elbow and wrist (with motion constrained at the shoulder) were observed with the forearm supinated: (1) wrist flexion-extension coordinated with elbow flexion-extension (an in-phase pattern) and (2) wrist flexion-extension coordinated with elbow extension-flexion (an antiphase pattern). At critical cycling frequencies, switching from antiphase to in-phase coordination was observed. Below a critical frequency the system was bistable, and above it only monostable. When the joints were in-phase, the end-effector trajectory was highly curved (a half-circle), and when the joints were antiphase, the end-effector trace was less curved (approaching a straight line). This suggests that the temporal dynamics of single-limb multijoint movement patterns may be examined under the influence of spatial constraints, e.g., the curvature of a required end-effector trajectory.

In this experiment, we study the 'ill-posed' problem of trajectory formation by examining the emergence (formation and change) of coordinative patterns between the elbow, wrist, and shoulder joints as the end-effector (hand) traces a series of two-dimensional (2D) arcs of monotonically varying curvature. By allowing motion about the shoulder (compared to Kelso et al. 1991), the limb is a redundant manipulator in this task with three degrees of freedom available for the production of a 2D trajectory. Answers to the following questions are sought: Which coordinative patterns are associated with trajectories demanding a specific curvature? Is the system characterized as multistable when spatial constraints are externally imposed? What are the system's *order parameters* or *collective variables* under such constraints? Are *df* recruited and suppressed in such a redundant system, and if so how and when?

2 Experiment

2.1 Subjects

A total of eight subjects, three female and five male adults, participated in this experiment. All eight subjects were right-handed, and seven were naive to the purpose of the experiment. The naive subjects received class credits for volunteering.

2.2 Experimental apparatus

The OPTOTRAK 3010 3D Motion Analysis System was used to record the x, y, and z displacement of nine infrared light-emitting diodes (IREDs) placed on the subject's right arm and torso. The OPTOTRAK 3010 camera consists of three one-dimensional sensors (anamorphic lenses) mounted in a single unit. Each sensor has a $34^\circ \times 34^\circ$ field of view, and the sensor array is precalibrated to a resolution of 0.1 mm in the x and y directions and 0.15 mm in the z direction at a distance of 2.5 m. The camera was mounted horizontally (approximately waist height), and subjects were seated approximately 2 m from the camera's central sensor with their right-hand side parallel to the OPTOTRAK camera's vertical plane of recording (Fig. 1A). The nine IREDs were placed in the following locations: (1) the acromian process; (2) below the lateral epicondyle; (3) posterior to the wrist radiocarpal joint; (4) at the end of a hand-held dowel; (5) the hip; (6 and 7) the forearm; and (8 and 9) the upper arm (Fig. 1B). The positioning of IREDs 6, 7, 8, and 9 allow for accurate reconstruction of the joint angles when the IREDs at the pivot points (joints) were occluded. The auditory metronome was generated with a computer (a 30-ms square wave pulse generated by a MAC II) and output through a loudspeaker mounted in front and to the left of the subject. The IRED signals were monitored, recorded, and stored on a DELL (466/M) PC, and the metronome signal was recorded with the OPTOTRAK/ODAU (analog to digital) device and also stored on the DELL PC. Both the IRED and metronome signals were recorded at a sampling frequency of 100 Hz.

2.3 Construction of curvature stimulus set, $\{\kappa_i\}$

The stimulus set $\{\kappa_i : i = 1 \ldots 6\}$ was 'subject specific' and a function of a self-paced 'curl movement' produced by the flexion-extension motion of the wrist and elbow in the sagittal plane, while shoulder motion and lateral movement of the elbow were minimized (Fig. 1B). The x, y, z trace of the end effector (IRED 4 in Fig. 1B) was recorded during the curl movement. The accumulated x, y trace points of IRED 4 formed an arc segment of a circle whose center (a, b) and curvature K_o were computed by minimizing the sum

$$\sigma^2 = \frac{1}{N} \sum_{k=1}^{N} (R_o - [(x_k - a)^2 + (y_k - b)^2]^{1/2})^2 \qquad (1)$$

over the parameters (a, b, R_o), where $R_o = 1/K_o$ and N is the number of data points. These parameters were used as a basis for constructing six similarly positioned arcs with curvatures $\kappa_i = i\delta\kappa$, $i = 1 \ldots 6$, where $\delta\kappa = K_o/6$. The curvature was chosen as the control parameter because (a) it provided perceptible differences between stimuli when scaled linearly, and (b) previous research (Kelso et al. 1991) showed that different stable interjoint patterns produced large curvature differences. To keep the distance traveled by the end effector constant for all κ, the angle $\Delta\alpha_i$ subtended by the arc was set so that the arc length $s^{(r)} = \Delta\alpha_i/\kappa_i$ was the same for all i. Each arc was similarly positioned in space by adjusting the center (a_i, b_i) so that it coincided with the basis arc.

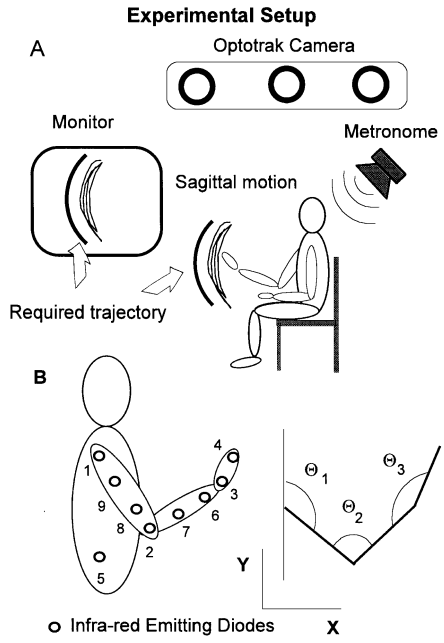

Fig. 1A. Position of the subject with respect to the OPTOTRAK camera and the computer displaying the required arcs. A diagram showing the placement of the nine infrared emitting diodes (IREDs) on the right arm is shown in **B**. The thin arc represents the x, y trace of the hand-held dowel used to compute K_o, and the stick figure portrays the orientation of the angles representing motion about the shoulder (θ_1), elbow (θ_2) and wrist (θ_3)

2.4 Task and procedures

Subjects traced the six arcs in two different conditions: (1) an increasing κ condition, in which the arcs were presented in the order $\kappa_1, \ldots \kappa_6$; and (2) a decreasing κ condition, in which arcs were presented in the order $\kappa_6, \ldots \kappa_1$. The arcs were displayed on a computer screen in such a way that arm movement and arc stimulus were as close as possible to being on parallel planes while still allowing for a clear view of the displayed arc (see Fig. 1A). Throughout a trial, the end-point trace of IRED 4 (the last 100 points) was juxtaposed with the stimulus arc. Each arc of a given curvature κ was presented for a total of 15 s, with 10 trials in each condition grouped into five-trial blocks. Each subject performed alternating condition blocks, and the initial condition was randomized across subjects. The movement of the end effector was

paced by the metronome at a required frequency of 1.0 Hz. In all, subjects produced a total of 90 cycles of motion per trial and 180 cycles of motion across both conditions.

After attaching the IRED to the right arm, we performed the calibration of the stimulus set $\{\kappa_i\}$. Next, we familiarized the subject with the relationship between motion about a joint and the end-point trajectory (IRED 4). To do this, we displayed the arc with maximum curvature, $\kappa_6 = K_o$, and had subjects flex and extend each joint. The effect of each joint's motion on the end-effector trace was pointed out to the subject. This procedure was repeated until we were confident that the subject understood how motion of their joints on the sagittal plane produced a trajectory of the hand on the computer screen. Subjects were then read the following three instructions: 'First, flex and extend the elbow, shoulder, and wrist in any combination you wish in order to trace the required arc; second, keep the joints on the sagittal plane, i.e., avoid lateral or medial movement of the elbow and hand; and third, trace the entire arc and maintain a 1:1 frequency relationship with the metronome by completing one full cycle (up and down) of motion per metronome beat.'

2.5 Data analysis

The reconstructed data set yielded 3D positions of the nine IREDs attached to the subject's right arm. From the line segments connecting the four pivot points in Fig. 1B, the shoulder angle (θ_1), elbow angle (θ_2), and wrist angle (θ_3) were calculated. Position and angle values were smoothed using a low-pass Butterworth filter (10 Hz). The following measures were computed as a function of curvature condition and stimulus curvature κ: (a) cycle durations of the y component of the end-point trace; (b) actual curvature $\kappa^{(o)}$ of the end-point trajectory; (c) actual end-effector travel distance $s^{(o)}$; (d) point estimates of elbow and wrist (ϕ_1) and elbow and shoulder (ϕ_2) relative phases from the angular time series; and (e) the power spectra of joint angular excursion.

To evaluate the subjects' temporal performance, the cycle duration of the y-component of the end-effector trajectory was computed using a peak picking algorithm. The peak-to-peak cycle durations τ within a trial for each subject were computed, where $\tau_n = 1, \ldots, n$ and n is the number of cycles in each trial. From these τ_n values, the cycling frequencies $f_n = 1/\tau_n$ were computed. The individual f_n values were averaged as a function of κ for each trial by condition and subject, and used as a measure of temporal tracking performance. Spatial performance consisted of two parts, reproducing an arc with curvature $\kappa_i^{(o)}$ equivalent to κ_i and maintaining a constant end-point travel distance $s^{(o)}$. The value of observed curvature, $\kappa^{(o)}$, was computed by fitting a circle (Eq. 1) to the xy-trace of the end-point trajectory, with the quantity $\kappa_i^{(o)} = 1/R_i^{(o)}$ taken as the produced curvature. For each κ_i, the mean travel distance, $s_i^{(o)}$, was obtained using the equation

$$s_i^{(o)} = \frac{1}{N_{1/2}} \sum_{n=1}^{N_{1/2}} \Delta s_n \qquad (2)$$

where Δs_n is the arc length of a complete half-cycle, defined as a segment of the trajectory between a minimum and maximum y-value, and $N_{1/2}$ is the total number of such half-cycles.

3 Results

3.1 Performance of temporal and spatial task requirements

Temporal performance. Shown in Table 1 are the mean cycle frequencies of the y-component of the end-effector trace for each subject as a function of curvature scaling direction. As a group, subjects reproduced the required frequency of 1.0 Hz most accurately for $\kappa_{4,5}$ (0.98 Hz) and least accurately for $\kappa_{1,6}$ (0.93 Hz and 0.95 Hz, respectively). Only subject MG was not within 10% of the required cycling frequency of 1.0 Hz, with the largest deviation occurring at $\kappa_{1,6}$ (0.8 and 0.77 Hz, respectively). The arc curvature by trial mean cycle frequencies were analyzed in a scaling direction (2) × arc curvature (6) ANOVA. Significant effects for arc curvature, $F(5, 35) = 3.0$, $P < 0.05$, and the scaling direction × arc curvature interaction, $F(5, 35) = 2.7$, $P < 0.05$, were found. Post-hoc tests ($P < 0.05$) of the arc curvature effect were all non-significant, with the largest difference being only 0.05 Hz between $\kappa_{4,5}$ and κ_1. The main effect most probably arose from the poor pacing behavior of subject MG compared with the other 7 subjects, especially for $\kappa_{1,6}$. Contrast tests ($P < 0.05$) of the interaction revealed significant differences between curvature conditions for $\kappa = \kappa_3, \kappa_4$, and κ_5, with the largest difference (only 0.03 Hz) between the two conditions occurring at κ_3. Given the small temporal differences between conditions, the above results demonstrate that seven of eight subjects accurately tracked the metronome with the end effector at the required frequency of 1 Hz for all κ values regardless of the direction of curvature scaling.

Spatial performance. Overall, subjects consistently changed the curvature of their end-effector trace in both the increasing and decreasing κ conditions (Fig. 2). There was a tendency in subjects to reproduce some required κs much better than others. For example, subjects SP, DF,

Table 1 Observed end-effector (y) frequency by subject and curvature condition

Subject:	SP	PT	CL	MG	MD	VZ	DF	MS
Dec κ	1.00	1.00	0.98	0.88	1.00	1.00	0.98	0.97
Inc κ	1.01	1.00	1.01	0.81	0.99	0.99	0.98	0.92

Fig. 2. The observed curvature $\kappa^{(o)}$ is plotted against the required curvature κ_i (where $i = 1 \ldots 6$) for the increasing (**A**) and decreasing (**B**) curvature conditions. The units on each axis correspond to $\kappa = 1/R$ where R is the radius of the required curve (*abscissa*) and the best fit radius of the observed curve (*ordinate*). Each *open square* represents the observed curvature $\kappa^{(o)}$ for a given κ_i, and there are ten values (ten trials) for each $\kappa^{(o)}$. The *diagonal line* represents a perfect fit between $\kappa^{(o)}$ and κ_i. In both **A** and **B**, the *arrows* depicted in the *second row* (*first column*) represent the direction of curvature change

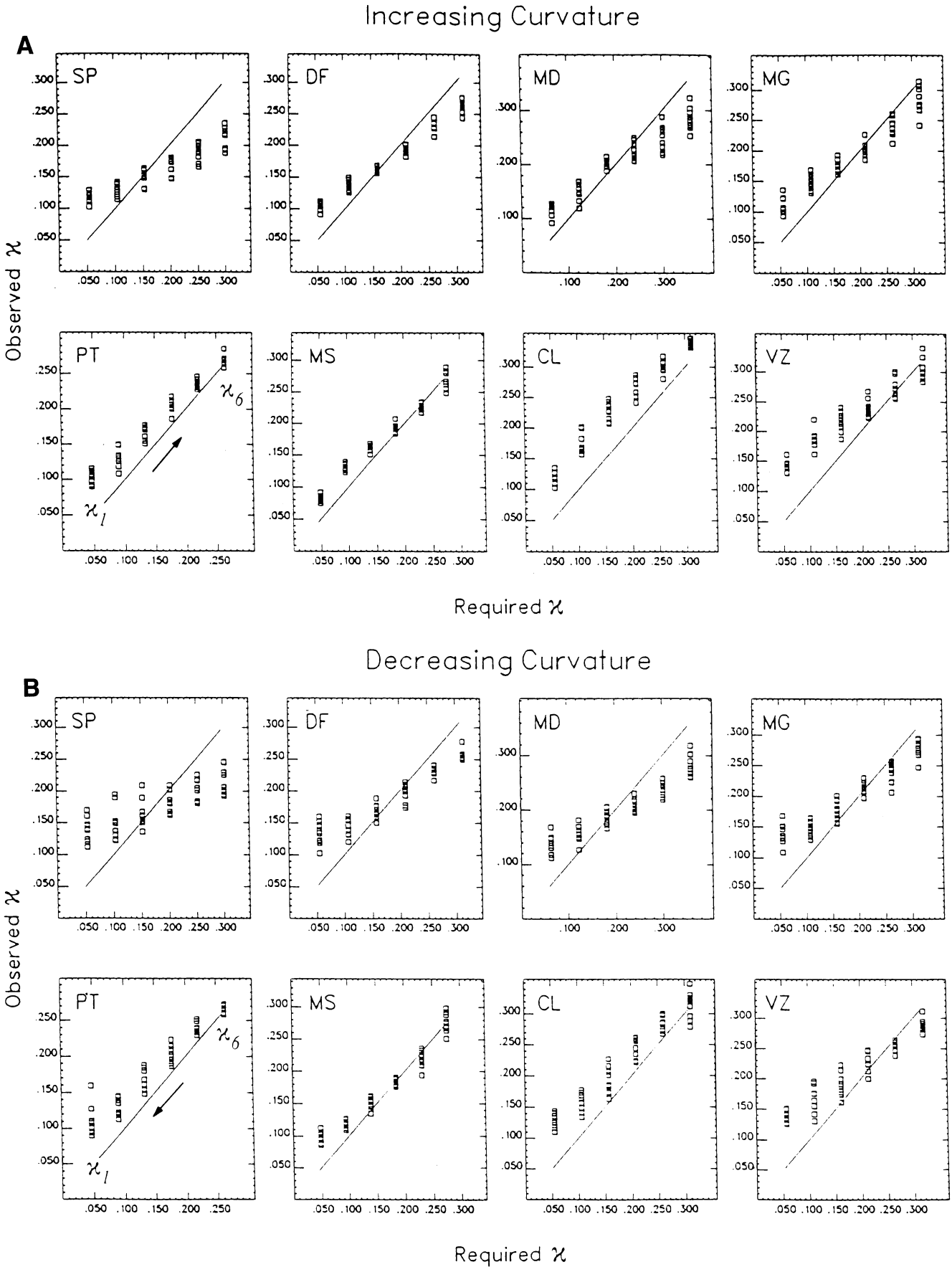
Increasing Curvature
A
SP
DF
MD
MG
PT
MS
CL
VZ
Observed κ
Required κ
Decreasing Curvature
B
SP
DF
MD
MG
PT
MS
CL
VZ
Observed κ
Required κ

Table 2. Comparison of the visual stimulus arc length, $s^{(r)}$, and the actual end-effector travel distance $s^{(o)}$ for the eight subjects under decreasing and increasing κ-condition

	SP	PT	CL	MG	MD	VZ	DF	MS
$s^{(r)}$	87	105	86	84	72	76	84	108
$s^{(o)}_{\text{dec }\kappa}$	78.9	80.5	63.1	63.7	48.7	52.4	58.2	71.4
$s^{(o)}_{\text{inc }\kappa}$	78.6	84.5	64.6	64.6	48.7	54.5	57.6	75.6

MD, and MG matched the intermediate κ values (κ_3, κ_4) quite well, but were less accurate in their productions of the high and low κ values (Fig. 2A, B, top row). The other four subjects, PT, MS, CL, and VZ, accurately reproduced the high κ values (κ_5, κ_6) more so than the intermediate or low κ values (Fig. 2A, B, bottom row). Even with these discrepancies, a linear regression of $\kappa_i^{(o)}$ on κ_i yielded $r^2 s > 0.9$ for all subjects except SP (Inc κ, $r^2 = 0.65$; Dec κ, $r^2 = 0.87$). The above results demonstrate that subjects performed the required task of producing a linear change in the curvature of the end-point trajectory.

The other spatial requirement in this task was to maintain a constant end-effector amplitude ($s^{(r)}$) as arc curvature was scaled. Table 2 reports the mean end-effector travel distances for each subject as a function of scaling condition (Inc κ, Dec κ). As the means show, each subject undershot their required amplitude $s^{(r)}$, with the distance traversed along the required arc ranging from 91% for subject SP to 66% for subjects MD and MS. The κ_i values of $|s^{(r)} - s_i^{(o)}|$ were analyzed for each subject separately in repeated measures ANOVAs with two levels of scaling direction and six levels of arc curvature, κ. Subject PT was the only subject to consistently traverse more of the arc in the increasing than the decreasing condition, $F(1, 2) = 6.4$, $P < 0.05$ (see Table 2). All six subjects undershot $s^{(r)}$ for all κ values regardless of the direction of curvature scaling, $Fs(5, 10) > 9.9$, $P < 0.05$. Seven of eight subjects traced less of the required arc for κ_6 and κ_1 and more of the required arc for κ_3 or κ_4. The largest difference in produced arc length across κ values was 9 cm for subjects SP and PT. Only subject VZ traced more of the arc for κ_6 compared to κ_1, with the difference between these two κ values being only 2 cm. Even though the length of the arcs subjects produced fell short of their required $s^{(r)}$, each subject maintained a fairly constant observed arc length $s^{(o)}$ across κ and scaling conditions.

3.2 Observed patterns and pattern switching

Multicomponent coordination may be accurately described by the relative phases of the components with respect to an arbitrarily chosen reference (see, e.g., Kelso 1984; Schöner 1990, 1994). In the present case, if the component amplitudes are ignored, such an approach sufficiently describes coordination tendencies among the joints. Since the present task involves positioning an end effector along a constrained path in space that is geometrically related to joint excursions, the amplitudes must play a role in specifying the movement patterns. The extent to which the amplitudes parameterize the intrinsic features of the tracing task, purely biomechanical effects excluded, is not well known. In theoretical studies of bimanual coordination, the inverse amplitude-frequency property of nonlinear oscillators is employed to effect coordinative changes (see, e.g., Haken et al. 1985; and part II). There, the main thrust is to explore purely temporal constraints on the coordination dynamics (i.e., behaviors adequately described by the relative phase variables). Here, however, it is possible that the amplitudes themselves may undergo bifurcations, i.e., active *df* are suppressed and quiescent *df* recruited (Kelso et al. 1993). This implies that shifts in an already established amplitude do not generally produce a different qualitative behavior, only the appearance or disappearance of a finite amplitude will do so. In classifying patterns and analyzing pattern change, we will focus on qualitative changes in the joint relative phases, ϕ_i, joint amplitudes, ρ_i, and joint frequency ratios, Ω_i.

A summary of the three basic coordinative patterns compiled from the phase, amplitude, and frequency behavior of the three joints for all eight subjects is given in Table 3. Here, ρ_1 and ρ_2 refer to the wrist and shoulder amplitudes, Ω_1 and Ω_2 represent the frequency ratios of the wrist and shoulder with respect to elbow, and ϕ_1 and ϕ_2 refer to the point estimates of relative phase between the elbow and wrist and elbow and shoulder. The additional shoulder-elbow phase relation $\phi_2^* = (0^\circ, 180^\circ)$ corresponds to 2:1 frequency entrainment between the elbow and shoulder (Figs. 3 and 4). The symbol ε indicates displacements too small to allow for coherent phase behavior and approximates a zero amplitude state in a component. High κ arcs are predominantly performed

Fig. 3. Plotted in **A** and **B** are complete trials from the data set of subject PT for the decreasing and increasing curvature conditions, respectively. The end-effector trace, joint angles (five cycles), and power spectra (over 15 cycles) are plotted from *left* to *right*, respectively, as a function of κ (*top* to *bottom*). In *column two*, the elbow time series is the *dotted line*, the wrist the *dashed line*, and the shoulder the *solid line*. The *dotted vertical line* in the power spectra in *columns 3* through *5* represents the metronome pacing frequency. The power spectra for each joint are scaled to the maximum value observed for that joint in that trial

Table 3. Pattern classificaion as a function of component amplitudes, frequency ratios, relative phases and arc curvature (variables defined in text)

Pattern	Component amplitudes		Frequency ratios		Relative phases			Arc curvature
	ρ_1	ρ_2	Ω_1	Ω_2	ϕ_1	ϕ_2	ϕ_2	κ
I	Finite	Finite	1:1	1:1 or 2:1	0°	0°	or 0°, 180°	κ_6 to κ_3
II	Finite	Finite	1:1	1:1 or 2:1	180°	0°	or 0°, 180°	κ_3 to κ_1
III	Finite	Finite	–	1:1 or 2:1	–	0°	or 0°, 180°	κ_4 to κ_1

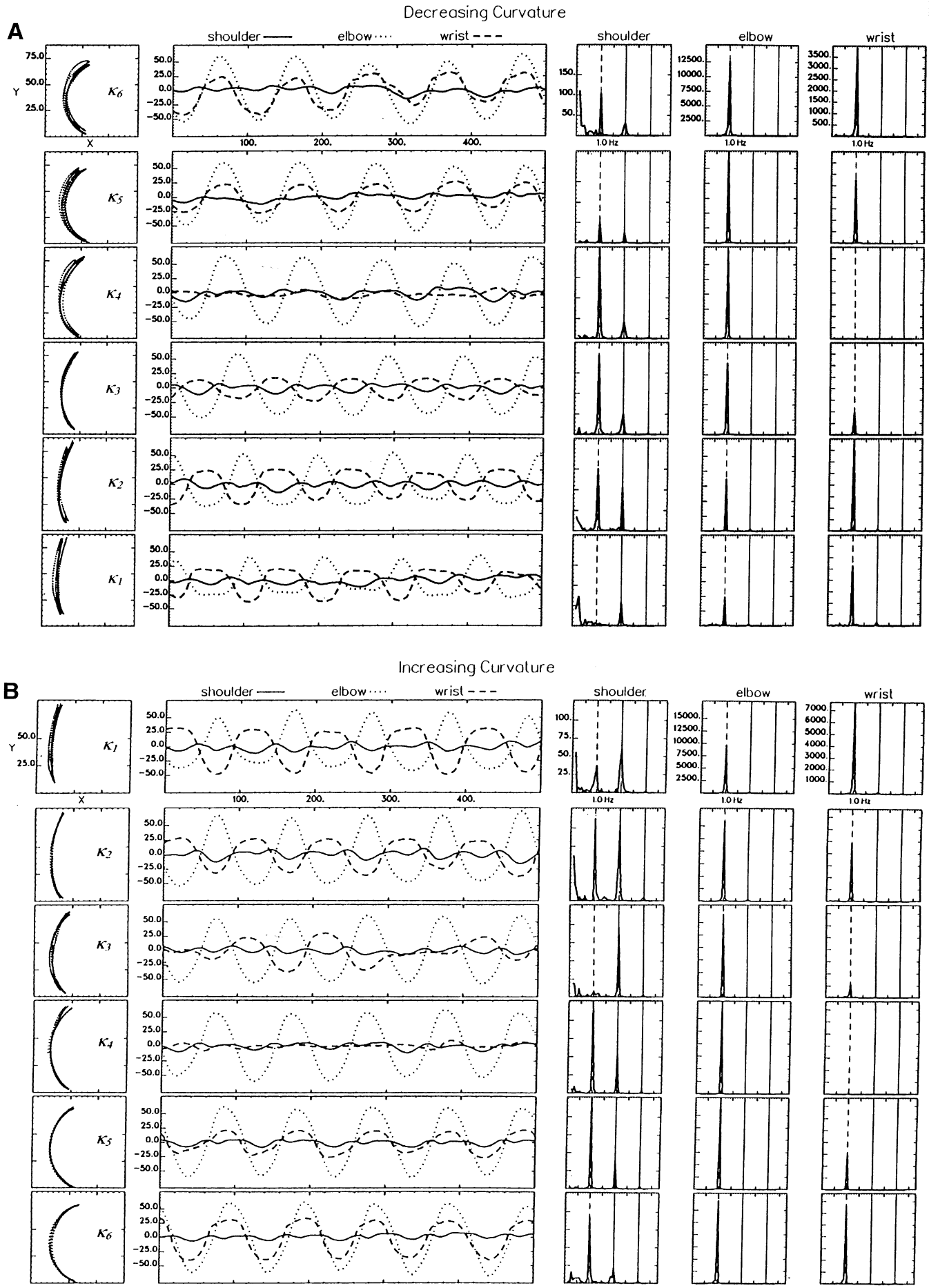
A
Decreasing Curvature
shoulder
elbow
wrist
K6
K5
K4
K3
K2
K1
1.0 Hz
B
Increasing Curvature
shoulder
elbow
wrist
K1
K2
K3
K4
K5
K6
1.0 Hz

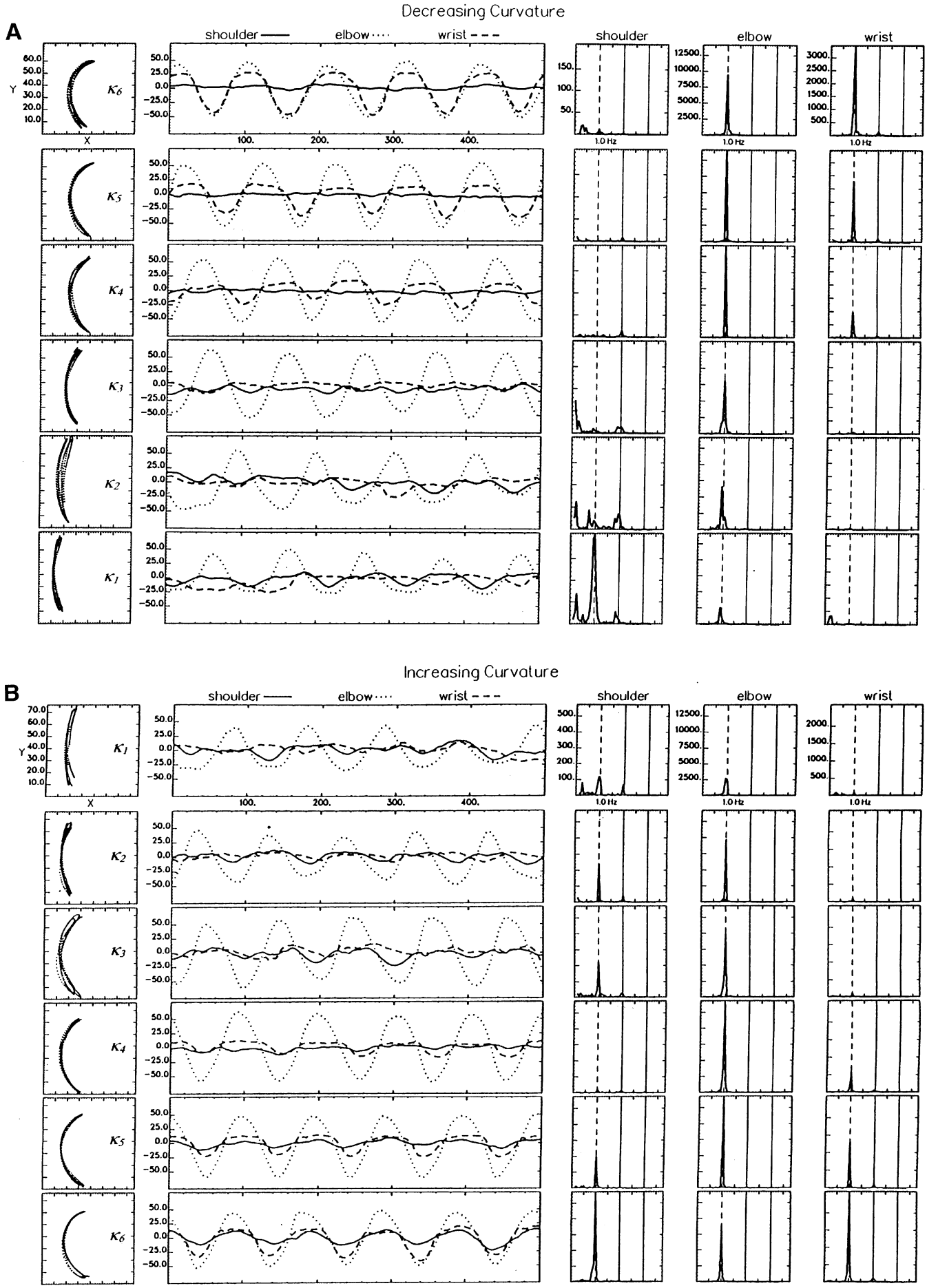
A
Decreasing Curvature
shoulder
elbow
wrist
K6
K5
K4
K3
K2
K1
1.0 Hz
B
Increasing Curvature
shoulder
elbow
wrist
K1
K2
K3
K4
K5
K6
1.0 Hz

with the wrist-elbow in-phase (pattern I), while low κ arcs are performed with the wrist-elbow antiphase (pattern II) or with no characteristic phase between these components (pattern III). Both of the Ω_2 frequency patterns occurred at all values of κ and did not seem dependent on any particular phasing, amplitude, or frequency relationship between the elbow and wrist.

Typical examples of observed coordination patterns and pattern changes are shown in Fig. 3 (subject PT) and Fig. 4 (subject CL). In Figs. 3A and 4A (column 2, row 1), the wrist and elbow amplitudes are well defined, and the observed oscillation is at the metronome frequency (columns 4 and 5). The coordination between the wrist and elbow is in-phase, $\phi_1 \approx 0^\circ$ (pattern I), in each trial for the high κ values. As arc curvature decreases, significant reductions in wrist amplitude occur in both trials at specific κ values ($\kappa = \kappa_4$ in Fig. 3A and $\kappa = \kappa_3$ in Fig. 4A). In Fig. 3A, wrist amplitude increases significantly at κ_3, and the elbow and wrist are attracted toward an antiphase pattern of coordination, $\phi_1 \approx 180^\circ$ (pattern II), which is maintained throughout the rest of the trial. In contrast, in Fig. 4A little or no increase in wrist amplitude occurs as κ continues to decrease beyond κ_3. Peaks in the wrist power spectra are noticeably absent. With wrist amplitude approaching zero, a characteristic phase between the elbow and wrist is no longer observed (pattern III). Clearly evident in the spectral plot shown in Fig. 4A (column 3) is the large increase in shoulder amplitude that occurs at κ_6. Such exchange in wrist (suppression) and shoulder (recruitment) motion represents a functional reorganization of the global pattern based on the task constraints of reproducing a changing arc curvature and maintaining a constant travel distance along the arc. In the increasing curvature condition (Figs. 3B and 4B), just the opposite type of behavioral changes occurs for both subjects. For subject PT (Fig. 1B), the initial phase between the elbow and wrist is $\phi_1 \approx 180^\circ$ (pattern II) when $\kappa = 1$. As arc curvature increases, wrist amplitude is suppressed at κ_4, and $\phi_1 \approx 180^\circ$ is no longer a stable attractive pattern. At κ_5, wrist motion is recruited with an attraction to $\phi_1 \approx 0^\circ$ (pattern I), a stable elbow-wrist phase pattern. In the case of subject CL (Fig. 4B), for κ_1 to κ_3, wrist motion is suppressed, and ϕ_1 has no characteristic value (pattern III). At κ_4, wrist amplitude increases, and ϕ_1 is attracted to a stable wrist-elbow phase pattern approximately equal to 0° (pattern I).

When $\rho_1 > \varepsilon$, wrist and elbow motion are always 1:1 frequency entrained regardless of the observed phase ($\phi_1 \approx 0^\circ$, 180°). Shoulder and elbow motion, however, exhibit frequency entrainment at a 2:1 ratio as well as a 1:1 ratio. The shoulder spectral plots of PT (column 3 in Fig. 3A, B) indicate a 2:1 frequency entrainment in Ω_2 for all κ. In the trials from subject CL (column 3, Fig. 4A, B), the shoulder and elbow are predominantly 1:1 frequency entrained with a few instances of 2:1 entrainment in Ω_2.

We created two subject groupings based on the type of pattern switching observed in the elbow-wrist phase relation, ϕ_1. Subjects in grouping 1 (SP, PT, MG, and MS) produced behavior consistent with that shown in Fig. 3, i.e., switching from in-phase (pattern I) to antiphase (pattern II) and vice versa around a point of minimal wrist amplitude. Subjects in grouping 2 (CL, MD, and DF) produced behavior consistent with that shown in Fig. 4, i.e., switching from in-phase (pattern I) to no characteristic phase (pattern III) in ϕ_1 when ρ_1 is small (Table 3). The data presented in Figs. 3 and 4 therefore contain the three basic features of the reproducible coordination effects in this experiment:[1] First, a discrete set of phase relationships when the component amplitudes are finite; second, significant changes (increases and decreases) in wrist and shoulder amplitude in the neighborhood of a critical κ_c; third, 2:1 and 1:1 shoulder-elbow frequency entrainment. The second feature was consistently associated with pattern change as a function of variation in the control parameter κ. For example, the amplitude reduction in ρ_1 may be considered transient when associated with a change in the value of ϕ_1 as in switching from $\phi_1 \approx 0^\circ$ to $\phi_1 \approx 180^\circ$ or vice versa (Fig. 3). When the reduction in ρ_1 persists in κ beyond the critical κ_c value, it may be considered a stable feature of the pattern (pattern III). Such is observed, for example, when the wrist and shoulder exchange roles and the burden of tracing the arc shifts solely to the shoulder-elbow pair (see Fig. 4). In the next two sections, we present a quantitative analysis of the data based on the above qualitative descriptions of interjoint coordination.

3.3 Joint amplitudes

As illustrated already, dramatic modulations (especially) in wrist and shoulder amplitude occurred simultaneously with pattern switching at specific κ values. In order to determine the relative role of each joint to the production of the observed arc, we computed ratio functions of the power in the wrist and shoulder with respect to the elbow. First, we performed an FFT on the joint angle time series as a function of κ (see columns 3–5 of Figs. 3 and 4). The relative power contributions from the wrist

Fig. 4. Complete trials from the decreasing (**A**) and increasing (**B**) curvature data sets of subject CL are plotted. The layout of the graphs is the same as in Fig. 3

[1] Although subject VZ's behavior in terms of frequency of motion, arc curvature, and end-point travel distance is consistent with the other subjects, we chose not to group this subject on the phase relation of ϕ_1 for the following reasons: The behavior of subject VZ, in general, may best be described as inconsistent with either grouping 1 or grouping 2 tendencies. In some instances, this subject demonstrated behavior similar to both groups of Subjects, i.e., in terms of phase and frequency characteristics. In many other instances, the behavior of this subject matched in no characteristic way the behavior of either group of subjects. For example, VZ displayed large modulations in wrist amplitude characterized by recruitment-suppression at all κ values. In fact, only subject VZ suppressed wrist motion for $\kappa = 6$, 5. Moreover, a consistent shift between antiphase and in-phase behavior between the elbow and wrist did not arise around the recruitment-suppression of wrist motion as in the other subjects

and the shoulder are given, respectively, by

$$w_{ij}(1) = \ln\left(\frac{W_{ij}^{\mathrm{wr}}}{W_{ij}^{\mathrm{el}}}\right) \tag{3}$$

$$w_{ij}(2) = \ln\left(\frac{W_{ij}^{\mathrm{sh}} + W_{ij}^{*\mathrm{sh}}}{W_{ij}^{\mathrm{el}}}\right) \tag{4}$$

where W_{ij}^{wr}, W_{ij}^{el}, and W_{ij}^{sh} are the spectral power for the wrist, elbow, and shoulder, respectively, at the subjects' pacing frequency (at or near the metronome frequency), i refers to the curvature index κ_i, and j is the number of trials (10) in each condition. When present, we also included the power at the first harmonic, $W_{ij}^{*\mathrm{sh}}$, as a contribution to shoulder motion. Based on the subject groupings outlined in Sect. 2.3 above, we averaged $w_{ij}(1)$ and $w_{ij}(2)$ [referred to now as $\bar{w}(1)$ and $\bar{w}(2)$] across subjects as a function of κ and condition. The mean data are plotted in Fig. 5A (group 1) and 5B (group 2).

Group 1 subjects. There are two main features of the data for subject group 1 plotted in Fig. 5A. First, in both the increasing and decreasing κ conditions, the value of $\bar{w}(1)$ is largest for the most (κ_6) and least (κ_1) curved arcs. These are the arcs associated with in-phase ($\phi_1 = 0^\circ$) and antiphase ($\phi_1 = 180^\circ$) coordination between the wrist and elbow. For the middle κ values, the value of $\bar{w}(1)$ is the smallest. These are the values of arc curvature associated with wrist suppression and loss of phase attraction between the elbow and wrist. An analysis of $\bar{w}(1)$ in a condition (2) × arc curvature (6) repeated measures ANOVA revealed no overall difference in $\bar{w}(1)$ as a function of direction of curvature change ($P > 0.05$), but it did reveal a strong effect of arc curvature, $F(5, 15) = 24.0$, $P < 0.01$. The results are clearly in line with the changes in $\bar{w}(1)$ shown in Fig. 5A. The second essential aspect of the data from group 1 subjects is that $\bar{w}(2)$ is fairly constant, except for κ_6 and κ_5 in the decreasing condition. The existence of just a few quantitative differences in $\bar{w}(2)$ are also statistically supported. An analysis of $\bar{w}(2)$ revealed no overall condition effect ($P > 0.05$), a small arc curvature effect, $F(5, 15) = 3.0$, $P < 0.05$, but a strong interaction effect, $F(5, 15) = 6.5$, $P < 0.01$. This interaction effect results from the difference in $\bar{w}(2)$ for κ_6 and κ_5 as a function of curvature condition. Only at these high required curvatures was a directional effect observed in the amplitude of shoulder motion.

Group 2 subjects. The single most important feature of the data for group 2 subjects is the change in the values of $\bar{w}(1)$ and $\bar{w}(2)$ around κ_3 and κ_4. As seen in Fig. 5B, the value of $\bar{w}(1)$ is largest for the most curved arcs and smallest for the least curved arcs ($\kappa_{1,2,3}$), while just the opposite occurs in $\bar{w}(2)$. The crossover of these values at κ_4 and κ_3 captures the exchange in component amplitude between the shoulder and wrist in these subjects. The values of $\bar{w}(1)$ and $\bar{w}(2)$ were analyzed in condition (2) × arc curvature (6) repeated measures ANOVAs. There were no significant differences found in $\bar{w}(1)$ or $\bar{w}(2)$ as a function of direction of curvature change ($ps > 0.1$). The curvature, $F(5, 15) > 8.1$, $ps < 0.01$, and condition × curvature interaction, $Fs(5, 15) > 7.9$, $P < 0.01$, effects were significant for both $\bar{w}(1)$ and $\bar{w}(2)$. Post-hoc tests ($P < 0.05$) of the curvature effect show that $\bar{w}(1)$ decreased significantly from κ_5 to κ_4, while $\bar{w}(2)$ increased significantly from κ_4 to κ_3. These significant shifts in $\bar{w}(1)$ and $\bar{w}(2)$ around κ_5, κ_4, and κ_3 capture the exchange in component amplitude occurring between the wrist and shoulder. Contrast tests of the condition × curvature interaction point to small differences between conditions when tracing the high curvature arcs, $\bar{w}(1)$ ($\kappa_{6,5,4}$) and $\bar{w}(2)$ ($\kappa_{6,5}$) (see Fig. 5B).

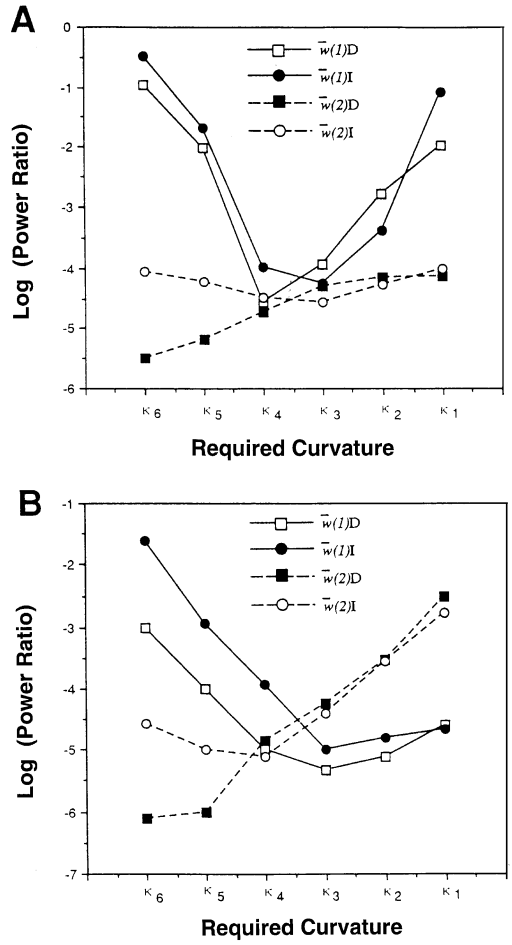

Fig. 5. Mean values of $\bar{w}(1)$ and $\bar{w}(2)$ are plotted as a function of κ for the two subject groupings: **A** group 1; and **B** group 2. The data from the decreasing condition should be read from *left* to *right* and the data from the increasing condition from *right* to *left*

3.4 Critical κ value: wrist recruitment-suppression

How consistently did subjects suppress wrist motion at a specific value of κ? Table 4 gives the number of trials as a function of subject grouping, scaling direction, and κ, where wrist amplitude dramatically changed. The critical κ value for subject group 1 corresponds to that value of κ where wrist motion was suppressed in both the increasing and decreasing κ scaling directions. This κ value is characterized by the lack of a prominent peak in the wrist joint power spectra at (or near) the required cycling frequency (see Fig. 3A, B, κ_4). For subject group 2, the

Table 4. Critical κ as a function of subject grouping and curvature condition

		Group 1				Group 2		
		SP	PT	MG	MS	CL	MD	DF
Dec κ	κ_5	–	–	1	–	–	9	1
	κ_4	8	9	7	2	6	1	6
	κ_3	2	1	2	6	3	–	1
	κ_2	–	–	–	2	1	–	2
Inc κ	κ_2	–	–	8	9	–	1	–
	κ_3	1	6	2	1	1	1	5
	κ_4	9	4	–	–	7	5	3
	κ_5	–	–	–	–	2	3	2

critical κ in the decreasing curvature condition is identified as the last curvature value in a trial where a prominent peak occurred in the wrist joint power spectra (see Fig. 4A, B, κ_4), while in the increasing condition, the critical κ is the first curvature value where a prominent peak in the wrist joint power spectra emerged (see Fig. 4B).

Subjects in group 1 suppressed wrist motion most often for $\kappa = 4$ and $\kappa = 3$ in the decreasing scaling condition, with subjects SP and PT producing similar behavior in the increasing condition. Subjects MG and MS tended to suppress wrist motion for smaller κ in the increasing compared with the decreasing condition. Overall, there is more variation in the κ value where wrist motion is suppressed and recruited in subjects in group 2 compared with subjects in group 1 in both scaling conditions. Examination of Table 4 clearly shows a lack of any strong hysteretic effect in the recruitment-suppression of wrist motion. Furthermore, the critical κ values for both subject groupings reflect the changes observed in $\bar{w}(1)$ reported in Sect. 3.3 (see Fig. 5). These critical κ values are used in the following section to align the mean phase and variability values of ϕ_1 and ϕ_2 in testing for significant changes in the phasing behavior near where the recruitment and suppression of wrist motion occurs.

3.5 Relative phase: pattern stability and loss of stability

Here we explore the relationship between component amplitude modulations and component phase measures around the critical curvature value κ_c. Is fluctuation enhancement present in $\phi_{1,2}$ before pattern switching? The means and standard deviations of ϕ_1 (elbow-wrist) and ϕ_2 (elbow-shoulder) were computed for each subject as a function of κ_i and trial. When there was a 2:1 frequency ratio between elbow and shoulder, the 0° phase values of ϕ_2^* (instead of 180°) were picked to maintain a consistent value in the mean, since 1:1 frequency entrainment between elbow and shoulder was characterized by a value of ϕ_2 near 0°. We aligned the mean and standard deviations as a function of the critical κ_c value for each subject grouping and averaged backwards (pretransition) and forwards (posttransition) around this point (see Buchanan and Kelso 1993; Kelso et al. 1986). The resultant mean values are plotted in Fig. 6 for group 1 and Fig. 7 for group 2.

Group 1 subjects. Two main features of the data in Fig. 6 bear directly on the amplitude data in Fig. 5A. First, on either side of κ_c, the value of ϕ_1 is either near 0° or 180° (Fig. 6A, C). These are the values of κ associated with the least and most curved arcs at which wrist amplitude is maximal (see Fig. 5A). Second, regardless of the direction of curvature change or initial coordinative pattern, the variability of ϕ_1 increases as κ_c is approached. In the decreasing curvature condition, the variability of the in-phase pattern, ϕ_{1sd}, increases as κ_c is approached (Fig. 6A); and in the increasing condition, a similar increase in ϕ_1 variability occurs in the antiphase pattern (Fig. 6C). After the switch in pattern, the variability of ϕ_1 decreases in both conditions. In general, the mean and variability of ϕ_2 for this subject grouping changed very little (Fig. 6B, D).

The mean values of ϕ_1 and ϕ_2 for group 1 subjects were analyzed by ANOVA with two levels of condition and six levels of plateau (three pretransition and three posttransition) for ϕ_1 and seven levels of plateau for ϕ_2 (three pretransition, three posttransition, and κ_c). The κ_c value of ϕ_1 is eliminated from the analysis due to the large reduction in wrist amplitude, making a computation of this measure unreliable, if not impossible (see Fig. 3A, B, κ_4). The values of ϕ_1 and ϕ_2 were aligned in such a manner that pretransition antiphase (Inc κ) and posttransition (Dec κ) antiphase behavior was compared, as was pretransition in-phase (Dec κ) and posttransition (Inc κ) in-phase behavior. Analysis of the means revealed no significant differences in the in-phase pattern as a function of direction of curvature change or distance from the transition plateau. The same result was obtained for the antiphase pattern ($Fs < 2.42$, $ps > 0.06$). This means that each pattern, when it is observed as an initial condition or a pattern that arose after wrist suppression-recruitment in κ_c, is the same across curvature conditions and κ (compare pre and post in-phase and antiphase patterns, Fig. 6A, C). The analysis also revealed that the value of ϕ_2 did not change significantly as a function of direction of curvature change or distance from the transition plateau ($Fs < 0.71$, $ps > 0.7$).

The variability data of ϕ_1 and ϕ_2 were aligned as described for the mean data. The values of ϕ_{1sd} were analyzed in an ANOVA with two levels of condition and six levels of plateau (three pretransition and three posttransition), and the values of ϕ_{2sd} were analyzed in an ANOVA with seven levels of plateau (three pretransition, three posttransition, and κ_c). The analysis revealed no significant difference in ϕ_{1sd} as a function of direction of curvature change ($F(1, 3) = 1.21$, $P > 0.03$). The value of ϕ_{1sd} did change significantly as a function of distance from the κ_c plateau, $F(5, 15) = 6.4$, $P < 0.01$, with a significant condition × plateau interaction also observed, $F(5, 15) = 6.4$, $P < 0.01$. Post-tests ($P < 0.05$) revealed that ϕ_{1sd} is largest before κ_c in the pretransition region, smallest for the least curved arcs, and increases significantly in the pretransition region as the system moves toward κ_c (Fig. 6A, C). Increases in ϕ_{1sd} before κ_c in the pretransition region for both the in-phase and antiphase pattern indicate fluctuation enhancement before wrist suppression. Decreases after κ_c in the posttransition

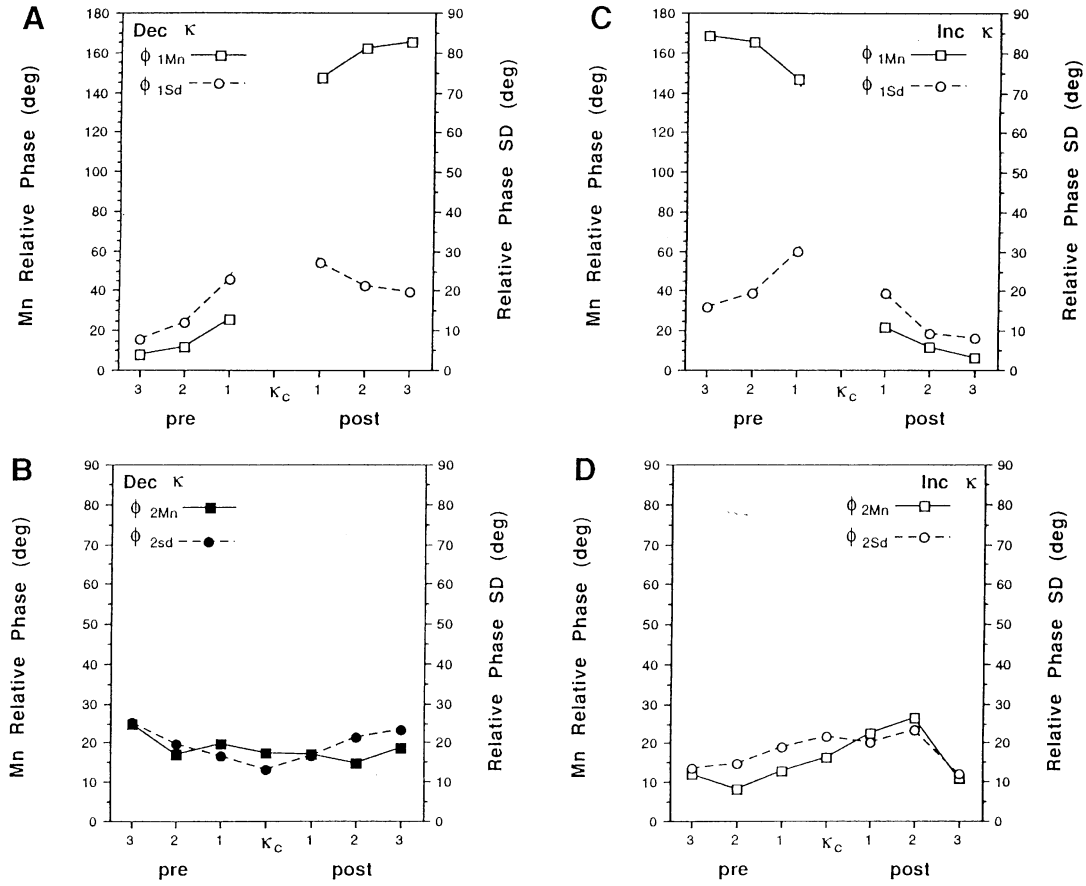

Fig. 6A–D. Relative phase means and variability of ϕ_1 (wrist-elbow phase) and ϕ_2 (shoulder-elbow phase) are plotted as a function of pre-and posttransition plateaus for group 1 subjects: **A** ϕ_1 for the decreasing condition; **B** ϕ_2 for the decreasing condition; **C** ϕ_1 for the increasing condition; **D** ϕ_2 for the increasing condition

region for both the in-phase and antiphase patterns represent an attraction to stable coordinative patterns with wrist recruitment. Contrast tests ($P < 0.05$) of the interaction revealed that the antiphase pattern, both before and after pattern switching, is more variable than the in-phase pattern. The value of ϕ_{2sd} did not change significantly as a function of direction of curvature change or distance from the κ_c plateau in the pre- and posttransition regions ($Fs < 0.65$, $ps > 0.6$).

Group 2 subjects. The changes that occur in ϕ_1 and ϕ_2 in group 2 subjects also correspond well with the amplitude changes for these subjects (see Fig. 5B). When a finite wrist amplitude is present (most curved arcs), wrist and elbow are close to in-phase behavior (Fig. 7A pre, C post) with low variability in ϕ_1. The shoulder and elbow (Fig. 7B, D) are also in-phase, but the variability of ϕ_2 is larger than that of ϕ_1, especially in the decreasing condition before κ_c. When the amplitude of the wrist is negligible for these subjects (least curved arcs), there is no characteristic phase between the elbow and wrist, and this is shown by the lack of data points in the post- and pretransition portions of Fig. 7A, C, respectively. Although wrist amplitude is suppressed for the least curved arcs in these subjects, shoulder amplitude is increased (see Fig. 5B). A very important aspect of the exchange in amplitude of these components is the simultaneous decrease in ϕ_2 variability in the decreasing curvature condition (Fig. 7B). In the increasing condition, the variability of ϕ_2 remains constant throughout.

The means and variability of ϕ_1 and ϕ_2 for group 2 subjects were analyzed by ANOVA with two levels of condition and four levels of plateau (three in-phase plateaus and κ_c) for ϕ_1 and seven levels of plateau (three pretransition, three posttransition, and κ_c) for ϕ_2. The value of ϕ_1 is eliminated from the analysis for values of $\kappa < \kappa_c$ due to the suppression of wrist amplitude, making computation of this measure highly unreliable (see Fig. 4A, B, κ_1). Analysis of the ϕ_1 means revealed a significant effect of condition, $F(1, 2) = 4.56$, $P < 0.01$. Overall, the value of ϕ_1 was larger in the decreasing condition ($\phi_1 = 40°$) then the increasing condition ($\phi_1 = 28°$). The plateau and condition × plateau interaction effects of ϕ_1 were significant ($Fs < 0.8$, $ps > 0.4$). The value of ϕ_2 did not change significantly as a function of curvature scaling direction (Dec $\kappa = 34°$ and Inc $\kappa = 27°$), $F(1, 2) = 2.81$, $P > 0.09$. A significant change in ϕ_2 emerged as a function of whether the wrist was active or suppressed, $F(6, 12) = 7.3$, $P < 0.01$. When the wrist was active for these subjects (Fig. 7B pre, 7D post), the value of ϕ_2 was

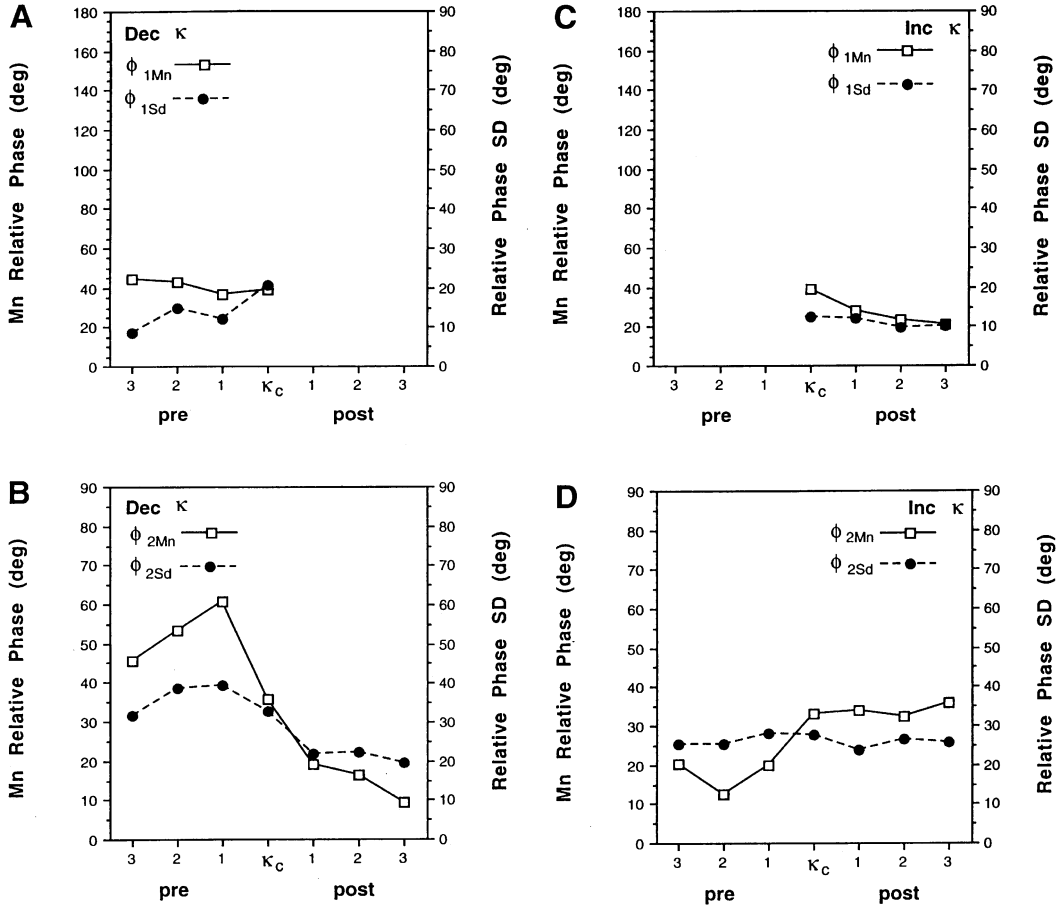

Fig. 7A–D. Relative phase means and variability of ϕ_1 (wrist-elbow phase) and ϕ_2 (shoulder-elbow phase) are plotted as a function of pre- and posttransition plateaus for group 2 subjects: **A** ϕ_1 for the decreasing condition; **B** ϕ_2 for the decreasing condition; **C** ϕ_1 for the increasing condition; **D** ϕ_2 for the increasing condition

around 40°, and when wrist motion was suppressed, the value of ϕ_2 was near 15° (Fig. 7B post, 7C pre).

The variability data of ϕ_1 and ϕ_2 were aligned relative to κ_c and analyzed by ANOVA as a function of pre- and posttransition position to the critical curvature plateau κ_c. Analysis of ϕ_{1sd} revealed significant effects of condition, $F(1, 2) = 4.2$, $P < 0.05$, plateau, $F(3, 6) = 4.7$, $P < 0.01$, and a condition × plateau interaction, $F(3, 6) = 3.2$, $P < 0.05$. Overall, the value of ϕ_{1sd} was larger in the decreasing (14°) than the increasing (11°) condition. Post-hoc tests ($P < 0.05$) of the plateau effect revealed that the value of ϕ_{1sd} in the κ_c plateau was significantly larger than the value of ϕ_1 in any of the other plateaus where wrist motion was present. Contrast tests ($P < 0.05$) of the interaction effect, however, showed that the value of ϕ_{1sd} in the critical curvature plateau (κ_c) in the decreasing condition was larger than the corresponding value in the critical curvature plateau in the increasing condition. With the low values of ϕ_{1sd} in the increasing condition across all plateaus where wrist motion occurs, this increase in the decreasing condition is evidence for fluctuation enhancement before wrist suppression. Analysis of ϕ_{2sd} revealed a significant plateau effect, $F(6, 12) = 2.42$, $P < 0.05$, and condition × plateau interaction, $F(6, 12) = 3.1$, $P < 0.05$. Post-hoc ($P < 0.05$) tests of the plateau effect did not reveal any significant differences. This effect probably arises from the larger values of ϕ_{2sd} when the wrist is active compared to when it is suppressed in the decreasing scaling condition. Such a shift represents a stabilization of shoulder-elbow motion with the suppression of wrist motion. Contrast tests ($P < 0.05$) of the interaction effect revealed that the variability in ϕ_{2sd} was larger in the decreasing condition than the increasing condition for the pretransition plateau (see Fig. 7B, D).

4 Discussion

Among the principle features of self-organizing systems are multistability, loss of stability before pattern switching, and hysteresis. Such features have been observed in a variety of coordination systems (see Kelso 1995 for review), many of which share three typical characteristics. First, frequency of motion is a control parameter that induces pattern switching. Second, the relative phasing ϕ between the components (whether fingers, limbs, or people) is an order parameter of the observed coordination dynamics in the sense of synergetics (Haken 1983). Third, the observed coordinative patterns can be

modeled as attractors of the order parameter's equations of motion (e.g., Haken et al. 1985; Schöner et al. 1986), with loss of stability identified as the generic mechanism of coordinative change. When critical fluctuations (e.g., Kelso and Scholz, 1985; Kelso et al. 1986) and critical slowing down (e.g., Buchanan and Kelso 1993; Scholz et al. 1987) in the order parameter accompany pattern switching, the behavior of the system is said to be self-organized (Haken 1983). Three aspects of the present data, namely, (1) pattern switching, (2) loss of stability, and (3) multistability, support the hypothesis that spatial trajectory formation is a self-organized process.

Systematic scaling of arc curvature induced pattern switching among the three joints in our experiment. In many temporal coordination tasks, transitions between patterns are typically abrupt with the same biomechanical components reorganized into a more stable pattern. Here, transitions between multijoint coordinative patterns also involved the recruitment and suppression of *df*. Quite similar processes, but very different behavioral outcomes characterized the two subject groupings. For example, in group 1 wrist amplitude decreased as the system entered the critical curvature zone and increased once the system left this region of parameter space. Pattern switching from in-phase ($\phi_1 \approx 0^\circ$) to antiphase ($\phi_1 \approx 180^\circ$) and vice versa between the elbow and wrist was not abrupt for these subjects. Instead, it was characterized by suppression and recruitment of wrist motion and corresponding annihilation of one phasing pattern followed by attraction to a different phasing pattern.

Similar processes, but different coordinative changes occurred in group 2. In the decreasing κ condition, wrist amplitude decreased significantly in the critical curvature region and remained depressed as arc curvature was further reduced. In the increasing curvature condition, wrist amplitude remained small, increasing once the system entered the critical curvature region. Suppression of wrist motion annihilated the elbow-wrist in-phase pattern in the decreasing curvature condition, while the recruitment of wrist motion led to an attraction to a stable in-phase pattern in the increasing condition. Just the opposite behavior was observed in the shoulder for these subjects. With the suppression of wrist motion, shoulder amplitude increased in the decreasing curvature condition; with recruitment of wrist motion, shoulder amplitude decreased in the increasing curvature condition. The behavior of these subjects takes the form of an exchange in component amplitudes around a critical curvature value.

Even though recruitment-suppression processes manifest themselves differently for each subject grouping, stability appears to be the key factor linking recruitment-suppression and pattern switching. In group 1 enhancement of fluctuations in ϕ_1 occurred before the suppression of wrist motion in the critical curvature region (see Fig. 6A, C, pretransition). With the recruitment of wrist motion, variability of ϕ_1 decreased as wrist and elbow found a stable relative phase relation, either $\phi_1 \approx 0^\circ$ or $\phi_1 \approx 180^\circ$ (see Fig. 6A, C, post). Even with such large modulations in wrist amplitude and changes in ϕ_1 variability, the coordination between elbow and shoulder remained quite stable for group 1 subjects (see Fig. 6C, D). Pattern switching takes the form of an exchange in stability or bidirectional switching between patterns as a function of arc curvature. Similar pattern switching results have been observed by Buchanan and Kelso (1993) for single-limb multijoint movements as a function of another spatially dependent control parameter, forearm orientation.

Stability also plays a part in the exchange of the contributions of the wrist and shoulder in group 2 subjects. In the decreasing curvature condition, ϕ_1 variability increased in the κ_c plateau before wrist suppression. With the suppression of wrist amplitude in the decreasing κ condition, shoulder amplitude increased with a drop in variability of ϕ_2. In this case, exchange of stability was between joint pairs and not between coordinative patterns within a joint pair. Thus, the exchange in stability involves the annihilation of a stable wrist-elbow phasing pattern with an attraction to a stable shoulder-elbow phase relation. With the recruitment of wrist motion at κ_c in the increasing curvature condition, the elbow and wrist motion were attracted to a stable in-phase pattern with a very low value of ϕ_{1sd} that changed little as κ continued to increase. Recruitment of wrist motion in the increasing condition was associated with little change in the variability of shoulder and elbow phase (see Fig. 7B, D).

Previous work has shown that in many temporally defined coordination tasks the system is multistable within specific regions of parameter space, i.e, two or more stable patterns of coordination coexist for the same value of cycling frequency (e.g., bimanual coordination, Kelso 1981, 1984; single-limb multijoint coordination, Kelso et al. 1991; perception-action coordination, Kelso et al. 1990; Wimmers et al. 1992). In this experiment, multistability is not so evident. Instead, within a certain region of parameter space, the system tends to exhibit monostability, at least with respect to the phasing between the elbow and wrist (group 1) or the exchange in active *df* as seen in the shoulder and wrist (group 2). However, across subject groupings, the system can be described as multistable, especially for the least curved arcs. Within this region of parameter space, as the previous discussion indicates, each subject grouping produces quite different coordination patterns utilizing different *df*.

Why is such diverse behavior across subject groupings observed? When available *df* are restricted to only those that are initially activated in a task, very consistent behavior in the form of multistability, loss of stability, and pattern switching occurs across subjects (see references in Introduction). In this experiment, the differences across subject groupings arise from the redundancy in the system, i.e., three joint *df* are available to perform a 2D task. Although the behavior across subject groupings is diverse, consistencies occur in the suppression of wrist motion, the attraction to stable phasing patterns, and 2:1 frequency entrainment between the shoulder and elbow. Thus, the dynamics of the behavior are consistent, even though individual differences are present. The bimanual experiment of Kelso et al. (1993) (see also Buchanan et al. 1997) described briefly in the Introduction is consistent with the differences in recruitment-

suppression processes observed in this experiment. In that experiment, all subjects exhibited transitions from the horizontal to the vertical motion plane, one group via a gradual recruitment of x and suppression of y motion, and another group via an abrupt transition exchange in x and y amplitudes. As in the present experiment, subjects fell predominantly into one or the other group, with only a few instances of crossover between groups. Many reasons may exist for such individual differences, physiological aspects, skill level, athletic ability, experience in specific prior tasks, etc. Our experiment, however, was not designed to address such individual differences, but only the consistencies in the coordination dynamics of trajectory formation among all subjects.

Taken together, the above three aspects of the data, pattern switching, loss of stability, and multistability, support the conclusion that arc curvature is a control parameter of the coordination dynamics governing trajectory formation. The data strongly support interjoint phasing as a relevant coordination variable or order parameter in this task. We also tested for significant changes in the variability of peak to valley displacement in all three joints (not presented here). Even though some significant changes in peak to valley displacement variation did arise in all three joints, consistent changes as a function of the critical curvature value did not emerge. Even though power spectra analysis and changes in phase around the critical curvature value are highly suggestive of joint amplitudes as an order parameter, direct results in terms of loss of stability did not arise. However, the data suggest that further study of the role of joint amplitudes in such tasks are worth exploring.

Interestingly, we observed two serendipitous findings in this experiment that highlight the flexibility of a redundant system in the production of spatial patterns of coordination. The first is associated with the 'bidirectional' nature of the transitions and the lack of hysteresis (see Table 4) in the elbow-wrist coordination patterns. One explanation for lack of hysteresis may be that the arcs provide very specific perceptual information about the contribution of the joints to the overall pattern. Instead of hysteresis, the system suppresses and recruits wrist and shoulder motion at very specific curvature values, κ_c.

Previous work by Warren (1984) has demonstrated a perceptual sensitivity to whether stairs are climbable or not based on the relationship between riser height and subject leg length. Such results point to intimate links between perception and inherent biomechanical properties of motor control (see also Warren, 1987). Viviani and colleagues have also demonstrated strong links between perception and action in single-limb multijoint movement tasks that require the tracing of ellipses (e.g., Viviani et al. 1987; Viviani and Mounoud 1990) and the perception of elliptical motion (Viviani and Stucchi 1993). Similar links between the production and perception of single-limb multijoint movements have been established by Kelso and Pandya (1990) (see also Haken et al. 1990). Likewise, in the context of learning (Zanone and Kelso 1992, 1994) and intentional switching (Kelso et al. 1988; Scholz and Kelso 1990), it has been demonstrated how specific information can constrain (and is constrained by) the coordination dynamics. Such results may pertain to the amplitude modifications observed in the wrist and shoulder. The critical κ_c arc may provide very specific information regarding the role (in terms of amplitude) of a given joint. This is seen, for example, in the relationship between minimum wrist amplitude, κ_c, and the exchange in stability of patterns in group 1 subjects. The same may be said for the relationship between wrist and shoulder amplitude and κ_c value for group 2 subjects. Lack of any hysteretic effects supports the contention that arc curvature carries very specific information with respect to joint amplitude.

A second unexpected result was the 2:1 frequency entrainment between the elbow and shoulder. For the least curved arc, the second peak in the shoulder was associated with maximum extension of the elbow. Shoulder flexion, at this point, can increase downward movement of the end effector, leading to a greater distance traveled along the required arc. However, such a clear relationship between distance traveled and the 2:1 frequency ratio was absent for high values of κ. Switching from 1:1 to 2:1 ratios and vice versa was also observed in the data of several subjects. Entrainment, loss of entrainment, and switching between frequency ratios (e.g., 1:2, 1:3, 4:3, etc.) in bimanual coordination tasks have been strongly linked to the stability of the temporal ratios (e.g., DeGuzman and Kelso 1991; Kelso and DeGuzman 1988; Peper et al. 1995; Treffner and Turvey 1993; Walter and Swinnen 1990, 1992). Based on the variability of ϕ_2, the production of 1:1 and 2:1 ratios cannot be directly linked to stability properties per se. These ratios may relate directly to the amplitude of the end-point trace or possibly to the recruitment and suppression of *df*, with some tie to pattern stability. The exact role of such frequency entrainment in single-limb multijoint movements, however, remains open to investigation.

In much of the experimental work on human coordination, the transitions between patterns have been shown to take the form of inverted pitchfork (e.g., Kelso 1984; Haken et al. 1985) or saddle-node (e.g., Jeka and Kelso 1995; Kelso et al. 1990) bifurcations, two of the generic forms of bifurcations observed in nonlinear dynamical systems (e.g., Kelso et al. 1994b; Thompson and Stewart 1986). Under conditions where the system has access to previously quiescent *df* or the possibility of freezing or removing an active *df*, then the recruitment or suppression of a *df* may take the form of a Hopf bifurcation. The Hopf bifurcation is a mechanism whereby biological systems can stabilize goal-directed actions by recruiting and suppressing task-specific *df* under changing environmental conditions (Kelso et al. 1993). The suppression and recruitment of wrist motion at κ_c is reminiscent of a Hopf-like bifurcation from a limit cycle to fixed point and vice versa, and as already stated, it is associated with pattern switching within and across joint pairs. This relationship suggests that the system can combine two flexible forms of coordinative modification, namely pattern switching and recruitment-suppression, to meet the demands of changing environmental conditions. To explore the above relationship, our results suggest that both spatial and temporal constraints on

single-limb multijoint movements and trajectory formation must be examined in unison. In part II (Deguzman et al. 1997), we provide a model that reproduces both the interjoint coordination effects, component amplitude effects, and resulting trajectories observed here as arc curvature is systematically varied as a control parameter.

Acknowledgements. Work supported by NIMH grant MH42900 and ONR grant N0014-92-J-1904. Preliminary results of this work were presented at the 24th Annual Society for Neuroscience Conference in Miami, Nov. 13–18, 1993.

References

Amazeen PG, Schmidt RC, Turvey MT (1995) Frequency detuning of the phase entrainment dynamics of visually coupled rhythmic movements. Biol Cybern 72:511–518

Asatryan DG, Feldman AG (1965) Functional tuning of the nervous system with control of movements or maintenance of a steady posture. I. Mechanographic analysis of the work of the joint on execution of a postural task. Biophysics 10:925–935

Bernstein NS (1967) The coordination and regulation of movements. Pergamon, Oxford

Buchanan JJ, Kelso JAS (1993) Posturally induced transitions in rhythmic multijoint limb movements. Exp Brain Res 94:131–142

Buchanan JJ, Kelso JAS, Deguzman GC, Ding M (1997) The recruitment and suppression of degrees of freedom in a bimanual rhythmic task. Hum Mov Sci 16:1–32

Carson RG, Goodman D, Kelso JAS, Elliot D (1995) Phase transitions and critical fluctuations in rhythmic coordination of ipsilateral hand and foot. J Mot Behav 27:211–224

DeGuzman GC, Kelso JAS (1991) Multifrequency behavioral patterns and the phase attractive circle map. Biol Cybern 64:485–495

DeGuzman GC, Kelso JAS, Buchanan JJ (1997) Self-organization of trajectory formation. II Theoretical model. Biol Cybern (in press)

Feldman AG (1986) Once more on the equilibrium-point hypothesis (λ model) for motor control. J Mot Behav 18:17–54

Grillner S (1975) Locomotion in vertebrates: central mechanisms and reflex interaction. Phys Res 55:247–304

Hass R, Fuchs A, Haken H, Horvath E, Kelso JAS (1991) Recognition of dynamic patterns by a synergetic computer. Prog Neur Net 3:341–359

Haken H (1983) Synergetics, an introduction: non-equilibrium phase transitions and self-organization in physics, chemistry and biology. Springer, Berlin Heidelberg New York

Haken H, Kelso JAS, Bunz H (1985) A theoretical model of phase transitions in human hand movements. Biol Cyern 51:347–356

Haken H, Kelso JAS, Fuchs A, Pandya A (1990) Dynamic pattern recognition of coordinated biological motion. Neur Net 3:395–401

Jeka JJ, Kelso JAS (1995) Manipulating symmetry in the coordination dynamics of human movement. J Exp Psychol Hum Percept Perform 21:360–374

Kelso JAS (1977) Motor control mechanisms underlying human movement reproduction. J Exp Psychol 3:529–543

Kelso JAS (1981) On the oscillatory basis of movement. Bull Psychon Soc 18:63

Kelso JAS (1984) Phase transitions and critical behavior in human bimanual coordination. Am J Physiol 15:R1000–R1004

Kelso JAS (1994) Elementary coordination dynamics. In: Swinnen S, Heuer H, Massion J, Casaer P (eds) Interlimb coordination: neural, dynamical and cognitive constraints. Academic Press, New York, pp 301–317

Kelso JAS (1995) Dynamic patterns: the self-organization of brain and behavior. MIT Press, Cambridge Mass.

Kelso JAS, DeGuzman GC (1988) Order in time: how cooperation between the hands informs the design of the brain. In: Haken H (ed) Neural and synergetic computers. Springer, Berlin Heidelberg New York, pp 180–196

Kelso JAS, Pandya AS (1990) Dynamic pattern generation and recognition. In: Badler N, Barsky B, Zelter D (eds) Making them move. Morgan Kaufmann, Calif., pp 171–190

Kelso JAS, Scholz JP (1985) Cooperative phenomena in biological motion. In: Haken H (ed) Complex systems: operational approaches in neurobiology, physical systems and computers. Springer, Berlin Heidelberg New York, pp 124–149

Kelso JAS, Southard DL, Goodman D (1979) On the nature of human interlimb coordination. Science 203:1029–1031

Kelso JAS, Scholz JP, Schöner G (1986) Non-equilibrium phase transitions in coordinated biological motion: critical fluctuations. Phys Lett A 118:279–284

Kelso JAS, Scholz JP, Schöner G (1988) Dynamics govern switching among patterns of coordination in biological movement. Phys Lett A 134:8–12

Kelso JAS, DelColle JD, Schöner G (1990) Action-perception as a pattern formation process. In: Jeannerod M (ed) Attention and performance XIII. Erlbaum, New Jersey, pp 39–169

Kelso JAS, Buchanan JJ, Wallace SA (1991) Order parameters for the neural organization of single, multijoint limb movement patterns. Exp Brain Res 85:432–444

Kelso JAS, Buchanan JJ, DeGuzman GC, Ding M (1993) Spontaneous recruitment and annihilation of degrees of freedom in biological coordination. Phys Lett A 179:364–371

Kelso JAS, Buchanan JJ, Murata T (1994a) Multifunctionality and switching in the coordination dynamics of reaching and grasping. Hum Mov Sci 13:63–94

Kelso JAS, Ding M, Schöner G (1994b) Dynamic pattern formation: a primer. In: Smith LB, Thelen E (eds) A dynamic systems approach to development. MIT Press, Cambridge, Mass., pp 13–50

Klein CA, Huang CH (1983) Review of pseudoinverse control for use with kinematically redundant manipulators. IEEE Trans SMC 13:245–289

Lacquaniti F, Soechting JF (1982) Coordination of arm and wrist motion during a reaching task. Neuroscience 2:399–408

Lacquaniti F, Soechting JF, Terzuolo SA (1986) Path constraints on point-to-point arm movements in three-dimensional space. Neuroscience 17:313–324

Latash ML (1993) Control of human movement. Human Kinetics Publishers, Champaign

Peper E, Beek P, Wieringen P van (1995) Multifrequency coordination in bimanual tapping: asymmetrical coupling and signs of supercriticality. J Exp Psychol Hum Percept Perform 21:1117–1138

Polit A, Bizzi E (1978) Processes controlling arm movements in monkeys. Science 201:1235–1237

Schmidt RC, Turvey MT (1994) Pulse-entrainment dynamics of visually coupled rhythmic movements. Biol Cybern 70:369–376

Schmidt RC, Carello C, Turvey MT (1990) Phase transitions and critical fluctuations in the visual coordination of rhythmic movements between people. J Exp Psychol Hum Percept Perform 16:27–247

Scholz JP, Kelso JAS (1990) Intentional switching between patterns of bimanual coordination is dependent on the intrinsic dynamics of the patterns. J Mot Behav 22:98–124

Scholz JP, Kelso JAS, Schöner G (1987) Non-equilibrium phase transitions in coordinated biological motion: critical slowing down and switching time. Phys. Lett A 123:390–394

Schöner G (1990) A dynamic theory of coordination of discrete movement. Biol Cybern 63:257–270

Schöner G (1994) From interlimb coordination to trajectory formation: common dynamical principles. In: Swinnen SP, Heuer H, Massion J, Casaer P (eds) Interlimb coordination: neural, dynamical and cognitive constraints. Academic Press, New York, pp 318–343

Schöner G, Kelso JAS (1988) Dynamic pattern generation in behavioral and neural systems. Science 239:1513–1520

Schöner G, Haken H, Kelso JAS (1986) A stochastic theory of phase transitions in human hand movement. Biol Cybern 53:442–452

Soechting JF, Lacquaniti F (1981) Invariant characteristics of a pointing movement in man. Neuroscience 1:710–720

Soechting JF, Terzuolo CA (1987a) Organization of arm movement is segmented. Neuroscience 23:39–52

Soechting JF, Terzuolo CA (1987b) Organization of arm movements in three dimensional space: wrist motion is piecewise planar. Neuroscience 23:53–61

Soechting JF, Lacquaniti F, Terzuolo CA (1986) Coordination of arm movements in three dimensional space, sensorimotor mapping during drawing movements. Neuroscience 17:295–311

Stein RG (1982) What muscle variables does the nervous system control. Behav Brain Sci 5:535–578
Thompson JMT, Stewart HB (1986) Nonlinear dynamics and chaos. John Wiley, New York
Treffner PJ, Turvey MT (1993) Resonance constraints on rhythmic movements. J Exp Psychol Hum Percept Perform 6:1221–1237
Treffner PJ, Turvey MT (1995) Handedness and the asymmetric dynamics of bimanual rhythmic coordination. J Exp Psychol Hum Percept Perform 21:318–333
Viviani P, Mounoud P (1990) Perceptuo-motor compatibility in pursuit tracking of two-dimensional movements. J Mot Behav 22:407–443
Viviani P, Stucchi N (1993) Biological movements look uniform: evidence of motor-perceptual interactions. J Exp Psychol Hum Percept Perform 18:603–623
Viviani P, Campadelli P, Mounoud P (1987) Visuo-manual pursuit tracking of human two-dimensional movements. J Exp Psychol Hum Percept Perform 13:62–78
Walter CB, Swinnen SP (1990) Kinetic attraction during bimanual coordination. J Mot Behav 22:451–473
Walter CB, Swinnen SP (1992) Adaptive tuning of interlimb attraction to facilitate bimanual decoupling, J Mot Behav 24:95–104
Warren WH (1984) Perceiving affordances: visual guidance of stair climbing. J Exp Psychol Hum Percept Perform 10:683–703
Warren WH (1987) Action modes and laws of control for the visual guidance of action. In: Meijer OG, Roth K (eds) Complex movement behavior: the motor-action controversy. Elsevier North Holland, Amsterdam, pp 339–380
Wimmers RH, Beek PJ, Wieringen PCW van (1992) Phase transitions in rhythmic tracking movements: a case of unilateral coupling. Hum Mov Soc 11:217–226
Zanone PG, Kelso JAS (1992) The evolution of behavioral attractors with learning: nonequilibrium phase transitions. J Exp Psychol Hum Percept Perform 18:403–421
Zanone PG, Kelso JAS (1994) The coordination dynamics of learning: theoretical structure and experimental agenda. In: Swinnen S, Heuer H, Massion J, Casaer P (eds) Interlimb coordination: neural, dynamical and cognitive constraints. Academic Press, New York, pp 461–490